THE JOURNAL OF BIOLOGICAL CHEMISTRY
Vol. 280, No. 35, Issue of September 2, pp. 30797–30806, 2005
Printed in U.S.A.

Phenotypic and Biochemical Analyses of BACE1- and BACE2-deficient Mice*[S]

Received for publication, May 12, 2005, and in revised form, June 27, 2005
Published, JBC Papers in Press, June 29, 2005, DOI 10.1074/jbc.M505249200

Diana Dominguez,[a,b] Jos Tournoy,[a,b] Dieter Hartmann,[a] Tobias Huth,[c] Kim Cryns,[d] Siska Deforce,[a] Lutgarde Serneels,[a] Ira Espuny Camacho,[a] Els Marjaux,[a,e] Katleen Craessaerts,[a] Anton J. M. Roebroek,[a] Michael Schwake,[f] Rudi D'Hooge,[g] Patricia Bach,[h] Ulrich Kalinke,[h] Dieder Moechars,[d] Christian Alzheimer,[c] Karina Reiss,[f] Paul Saftig,[f,i] and Bart De Strooper[a,j]

From the [a]Center for Human Genetics, Katholieke Universiteit Leuven and Flanders Interuniversity Institute for Biotechnology VIB4, Herestraat 49, 3000 Leuven, Belgium, the [f]Department of Biochemistry, University Kiel, Eduard-Buchner-Haus, Otto-Hahn-Platz 9, D-24118 Kiel, Germany, [d]Johnson & Johnson Pharmaceutical Research and Development, Turnhoutseweg 30, B-2340 Beerse, Belgium, the [g]Laboratory of Biological Psychology, Katholieke Universiteit Leuven, Tiensestraat 102, B-3000 Leuven, Belgium, the [c]Department of Physiology, University Kiel, Olshausenstrasse 40, D-24098 Kiel, Germany, and the [h]Division of Immunology, Paul Ehrlich Institute, Paul-Ehrlich-Strasse 51–59, D-63225 Langen, Germany

β-Secretase (BACE1) is the rate-limiting protease for the generation of the amyloid β-peptide (Aβ) in Alzheimer disease. Mice in which the *bace1* gene is inactivated are reported to be healthy. However, the presence of a homologous gene encoding BACE2 raises the possibility of compensatory mechanisms. Therefore, we have generated *bace1*, *bace2*, and double knockout mice. We report here that BACE1 mice display a complex phenotype. A variable but significant number of BACE1 offspring died in the first weeks after birth. The surviving mice remained smaller than their littermate controls and presented a hyperactive behavior. Electrophysiologically, subtle alterations in the steady-state inactivation of voltage-gated sodium channels in BACE1-deficient neurons were observed. In contrast, *bace2* knockout mice displayed an overall healthy phenotype. However, a combined deficiency of BACE2 and BACE1 enhanced the *bace1*$^{-/-}$ lethality phenotype. At the biochemical level, we have confirmed that BACE1 deficiency results in an almost complete block of Aβ generation in neurons, but not in glia. As glia are 10 times more abundant in brain compared with neurons, our data indicate that BACE2 could indeed contribute to Aβ generation in the brains of Alzheimer disease and, in particular, Down syndrome patients. In conclusion, our data challenge the general idea of BACE1 as a safe drug target and call for some caution when claiming that no major side effects should be expected from blocking BACE1 activity.

Alzheimer disease (AD)[1] is the most common cause of dementia for which neither a good diagnostic test nor an effective treatment is available yet. The most widely accepted hypothesis states that AD is initially triggered by the abnormal accumulation and possibly deposition of the small amyloid β-peptide (Aβ) in different brain regions, which in turn initiates a pathogenic cascade that ultimately leads to neuronal death, AD pathology, and dementia. Aβ is cleaved from a long membrane-bound precursor, the amyloid precursor protein (APP), by two consecutive cleavages. β- and γ-secretases are the enzymes that liberate the N and C termini of Aβ, respectively, and are the subject of intense investigation because of their relevance as candidate therapeutic targets to treat AD.

BACE1 and BACE2 are two highly homologous membrane-bound aspartyl proteases that can process APP at the β-secretase site (1–8). Although both enzymes exhibit many of the characteristics expected for β-secretase, it has been quite convincingly demonstrated that BACE1 is in fact the major β-secretase responsible for Aβ generation in brain (9–11). Contrary to BACE1, BACE2 is more highly expressed in peripheral tissues, but also to some extent in brain (2, 8, 12, 13), raising the question of whether BACE2 could contribute to the generation of the brain Aβ pool. Both BACE1 and BACE2 can cleave APP *in vitro* not only at Asp[1] (numbering considering the first amino acid of Aβ as position 1), but also at internal sites within the Aβ region. BACE1 cleaves between amino acids 10 and 11 of Aβ, resulting in an N-terminally truncated peptide that is considered more amyloidogenic and more neurotoxic than full-length Aβ (14) and that has been observed in senile plaques (15, 16). The internal BACE2 cleavage site is between amino acids 19 and 20 (8, 17, 18), and the resulting Aβ has thus far not been found in senile plaques. Moreover, BACE2-transfected cells produce reduced levels of Aβ (2, 8, 13, 18), and selective knockdown of endogenous BACE2 in human embryonic kidney 293 cells by RNA interference elevates Aβ secretion (19). These observations led to the suggestion that BACE2 does not function as a β-secretase, but rather as an α-like secretase that precludes Aβ formation (17–20). However, these *in vitro* observations cannot rule out a possible contribution of BACE2 to the

* This work was supported in part by a pioneer award from the Alzheimer Association (to B. D. S.); an Alzheimer Forschungsinititative (to D. D. and K. R.); the Fund for Scientific Research, Flanders; Katholieke Universiteit Leuven Project GOA; European Union APOPIS Contract LSHM-CT-2003-503330; Interuniversity Attraction Poles Program P5/19 of the Belgian Federal Science Policy Office (to B. D. S. and P. S.); and Grant IUAP P5/19 from the Federal Office for Scientific Affairs, Belgium. The costs of publication of this article were defrayed in part by the payment of page charges. This article must therefore be hereby marked "*advertisement*" in accordance with 18 U.S.C. Section 1734 solely to indicate this fact.

[S] The on-line version of this article (available at http://www.jbc.org) contains supplemental "Experimental Procedures," Refs. 1–3, and Figs. 1–5.

[b] Both authors contributed equally to this work.
[e] Recipient of the Fund for Scientific Research, Flanders.
[i] To whom correspondence may be addressed: Biochemisches Institut Christian-Albrechts-Universität Kiel, Olshausenstr. 40, D-24098 Kiel, Germany. Tel.: 49-431-8802216; Fax: 49-431-8802238; E-mail: psaftig@biochem.uni-kiel.de.
[j] To whom correspondence may be addressed. Tel.: 32-16-346-227; Fax: 32-16-347-181; E-mail: bart.destrooper@med.kuleuven.ac.be.

[1] The abbreviations used are: AD, Alzheimer disease; Aβ, amyloid β-peptide; APP, amyloid precursor protein; SFV, Semliki Forest virus; APPwt, wild-type APP; APPsw, Swedish APP mutation; APPfl, Flemish APP mutation; MEM, minimal essential medium; VSV, vesicular stomatitis virus.

Aβ pool in brain, and it has even been suggested that BACE2-mediated APP cleavage might play a role in the development of AD in individuals carrying the Flemish familial AD mutation in APP (8) as well as in the AD-like disease associated with Down syndrome (12, 21).

From a therapeutic point of view, there are increasing concerns with using γ-secretase inhibitors to treat AD. γ-Secretase processes a growing number of membrane proteins, and blocking their cleavage is likely to have toxic side effects. Indeed, administration of a potent γ-secretase inhibitor to mice results in marked defects in lymphocyte development and in intestinal villi and mucosa (22), as was also observed in presenilin-deficient mice (23). In contrast, BACE1 appears to be a promising drug target because genetic ablation of the *bace1* gene in mice does not seem to be associated with any gross abnormality (9–11). Moreover, BACE1 deficiency could prevent the learning and memory impairments and the cholinergic dysfunction observed in a transgenic mouse model for AD (24). Although BACE1 function might still be required under particular conditions that may have escaped detection, these results highlight BACE1 as one of the best available drug targets for AD. At this point, however, it cannot be excluded that BACE1 has important functions *in vivo* and that the apparent lack of phenotype in *bace1* knockout mice is due to the activation of compensatory mechanisms or to genetic redundancy. Because of their high homology, BACE2 is the best candidate protease to compensate for the absence of BACE1 function. Based on this homology, it is also likely that active-site inhibitors for BACE1 will affect, in addition, BACE2 protease activity.

To better understand the biological functions of BACE1 and BACE2, to analyze possible overlapping functions of these two proteases, and to attempt to predict the consequences of blocking BACE function *in vivo*, we generated mice with inactivated *bace1* and/or *bace2* genes. Unexpectedly and in contrast to what has been published for *bace1* knockout mice, we observed a phenotype associated with BACE1 deficiency, *viz.* a higher mortality rate early in life. *bace2* knockout mice were fertile and viable, with no major phenotypic alteration. Most important, mice with inactivated *bace1* and *bace2* genes were fertile and viable, but presented neonatal mortality that was even higher than that of the monogenic *bace1* line. These results suggest that BACE2 indeed partially compensates for the absence of BACE1 in *bace1* knockout mice and that therapeutic inhibition of BACE function may result in adverse side effects.

EXPERIMENTAL PROCEDURES

Antibodies—The C terminus-specific antibody for mouse BACE1 (B48) was raised in New Zealand White rabbits using synthetic peptide CLRHQHDDFADDISLLK. Rabbit antibodies B7/8 raised against Aβ (25) and B63 raised against the C terminus of human APP (26) have been described. Anti-FLAG monoclonal antibody was from Sigma. The N terminus-specific antibody for human Aβ (82E1) was from IBL Co., Ltd. (Tokyo, Japan).

Plasmid Construction—cDNAs to be expressed in non-neuronal cells were subcloned into a derivative of the eukaryotic expression vector pSG5 (Stratagene) that contains a larger polylinker (pSG5**; polylinker EcoRI, SpeI, SacII, HindIII, NotI, XhoI, SmaI, SacI, BamHI, and BglII). BACE1 cDNA was amplified from mouse brain RNA using primers 5′-GGATTCATGGCCCCAGCGCTGCACTGGCT-3′ and 5′-GAGCTCTCACTTGAGCAGGGAGATGTCATC-3′ (with the SacI site underlined) and directly cloned into pGEM-T (Promega). The SacI-SacII fragment was subsequently subcloned into the SacI-SacII sites of pSG5**. BACE2 cDNA was amplified from mouse pancreas cDNA using primers 5′-ATGGGCGCGCTGCTTCGAGCAC-3′ and 5′-TCATTTC-CAGCGATGTCTGAC-3′ and cloned into the pGEM-T vector. The XmaIII fragment of pGEM-T-mBACE2 was subsequently subcloned into the SmaI site of pSG5**. For cloning of BACE2 cDNA containing a deletion of exon 6 (BACE2ΔE6), two subfragments of the cDNA were separately amplified using primers that contain the deletion. The 5′-fragment was amplified using T7 as the forward primer and 5′-AGAAAACTCTGGAATCTCTCTGCAGTCCAGGTTGAGGTTCTGG-3′ as the reverse primer. The 3′-fragment was amplified using primers 5′-CTGGACTGCAGAGAGATTCCAGAGTTTTCTGATGGCTTCTGGA-C-3′ and 5′-GCTGCAATAAACAAGTTCTGCT-3′. The purified 5′- and 3′-subfragments were mixed together and PCR-amplified using the T7 and 5′-GCTGCAATAAACAAGTTCTGCT-3′ primers. The PCR product was digested with EcoRI and BamHI and cloned into the same sites of pSG5**. Cloning of bace2 and bace2ΔE6 containing a C-terminal FLAG epitope was done by PCR amplification on pSG5**BACE2 and pSG5**-BACE2ΔE6, respectively, using primers 5′-CGGAATTCCACCATGGG-CGCGCTGCTTCGAGCA-3′ (with the EcoRI site underlined) and 5′-C-GGGATCCTCA*TTTATCGTCGTCATCCTTGTAGTC*TTTCCAGCGAT-GTCTGACTAGT-3′ (with the BamHI site underlined and the FLAG epitope in italics). PCR products were digested with EcoRI-BamHI and cloned into the same sites of the pSG5** vector. All constructs were verified by sequencing.

For expression in neuronal and glial cells, cDNAs were cloned into Semliki Forest virus (SFV) type 1. Cloning of SFV-APPwt, SFV-APPsw, and SFV-APPfl has been described previously (27, 28).

Primary Cultures and Cell Lines—Medium, serum, and supplements for maintenance of cells were obtained from Invitrogen. COS cells and adult mice fibroblasts were maintained in Dulbecco's modified Eagle's medium/nutrient mixture F-12 (1:1) supplemented with 10% fetal calf serum. Primary neuronal cultures were generated from trypsinized brains obtained from day 14 embryos and maintained in Neurobasal medium (Invitrogen) supplemented with B27 and 0.5 μM L-glutamine. Cytosine arabinoside (5 μM) was added 24 h after plating to prevent non-neuronal (glial) cell proliferation. For glial cell cultures, Neurobasal medium was replaced with minimal essential medium (MEM; Invitrogen) supplemented with 10% horse serum, 0.225% $NaHCO_3$, 2 mM L-glutamine, and 0.6% glucose (MEM-HS). Cultures were maintained at 37 °C in a humidified 5% CO_2 atmosphere.

DNA Transfer and Metabolic Labeling—COS cells were plated in 6-cm^2 plates 1 day before transfection. Approximately 70–80% confluent cells were transfected with a total of 2 μg of DNA (1 μg of APP and 1 μg of BACE plasmids) and 6 μl of FuGene 6 (Roche Applied Science). Two days after transfection, cells were metabolically labeled with 100 μCi/ml [^{35}S]methionine for 4 h; the conditioned medium was collected; and cells were directly lysed in double immunoprecipitation assay buffer (50 mM Tris-HCl (pH 7.8), 150 mM NaCl, 1% Triton X-100, 1% sodium deoxycholate, and 0.1% SDS).

Neurons were maintained in Neurobasal medium, and ~48 h after the addition of cytosine arabinoside, they were infected with recombinant SFV. Glial cells were maintained for ~1 week in MEM-HS, passaged at least once, and infected with recombinant SFV ~48 h after trypsinization. (This treatment ensured the absence of neurons in the culture.) For both neurons and glial cells, a 10-fold dilution of SFV encoding APPwt, APPsw, or APPfl was added to the cultures, and infection was allowed to proceed for 1 h. The conditioned medium containing the virus was then replaced with fresh medium, and cells were further incubated for 2 h. Cells were metabolically labeled with 100 μCi/ml [^{35}S]methionine for 4 h; the conditioned medium was collected; and the cells were directly lysed in double immunoprecipitation assay buffer.

Mouse fibroblasts were plated in 12-well plates 1 day before infection (~300,000 cells/well). A 1:4 dilution of adenovirus encoding APPsw was added to the medium, and cells were further incubated for 48 h. Metabolic labeling was subsequently done as described above.

Analysis of APP Processing—Full-length APP and C-terminal fragments were immunoprecipitated from cell extracts using antibody B63. Aβ was immunoprecipitated from the conditioned medium using antibody B7/8. Protein G-Sepharose beads (Amersham Biosciences) were added to the mixtures, followed by overnight incubation at 4 °C with rotation. The immunoprecipitates were washed five times with double immunoprecipitation assay buffer and once with 0.3× Tris-buffered saline and then solubilized with NuPAGE lithium dodecyl sulfate loading buffer. Samples were heated for 10 min at 70 °C and electrophoresed on 4–12% precast gels (Novex). Radiolabeled bands were detected using a PhosphorImager (Amersham Biosciences).

Analysis of APP Processing Using Antibody 82E1—Neurons and glial cells were infected with recombinant SFV for 1 h as described above. The medium was subsequently replaced with Neurobasal medium (neurons) or MEM-HS (glial cells), and cells were further incubated for 6 h. Cells were lysed in phosphate-buffered saline containing protease inhibitors (Trasylol, 1 μg/ml pepstatin, and 5 mM EDTA) and 1% Triton X-100. Samples of cell extracts were resolved by SDS-PAGE and probed with antibody B63. Aβ was immunoprecipitated from the conditioned

medium using antibody B7/8 and detected by Western blotting using antibody 82E1.

Fluorescence Resonance Energy Transfer Analysis—COS cells were transfected with 2 μg of either empty vector or vector encoding BACE1-FLAG, BACE2-FLAG, or BACE2ΔE6-FLAG using 6 μl of FuGene 6. Forty-eight hours after transfection, cells were scraped in buffer containing 5 mM Tris (pH 7.4), 250 mM sucrose, 1 mM EGTA, and 1% Triton X-100, and protein concentration was determined using Bio-Rad protein assay dye reagent. Proteins (~400 μg) were subsequently incubated overnight at 4 °C with antibody B48 (BACE1-transfected cells) or anti-FLAG antibody (BACE2-transfected cells) and protein G-Sepharose beads. The immunoprecipitates were washed three times with Tris-buffered saline containing 0.1% Triton X-100 and twice with Tris-buffered saline. BACE activity was subsequently measured in an *in vitro* assay (Panvera P2985) by fluorescence resonance energy transfer according to the manufacturer's instructions. Briefly, an APP-based peptide substrate carrying the Swedish mutation and containing a fluorescence donor and a quencher acceptor at each end was used. The intact substrate is weakly fluorescent and becomes highly fluorescent upon enzymatic cleavage. BACE immunoprecipitates were directly resuspended in 20 μl of assay buffer provided with the kit, and after substrate addition, excitation and emission were measured using VICTOR^2 (PerkinElmer Life Sciences Model 1420 multilabel counter).

Pup Exchange—A total of eight BACE1 homozygous and eight wild-type couples were used for the experiment. Coupling was synchronized, and pups were exchanged during the first day of birth. The number of pups was followed until weaning.

Electrophysiological Recordings—Acutely isolated pyramidal cell somata were prepared from the sensorimotor cortex of anesthetized and then decapitated wild-type and *bace1*$^{-/-}$ mice (23–30 days of age) using an established method of combined enzymatic/mechanic dissociation (29). Briefly, freshly prepared neocortical slices were incubated for 30 min in warmed (29 °C) artificial cerebrospinal fluid and then maintained at room temperature. Artificial cerebrospinal fluid was constantly gassed with 95% O_2 and 5% CO_2 and contained 125 mM NaCl, 3 mM KCl, 2 mM $CaCl_2$, 2 mM $MgCl_2$, 1.25 mM NaH_2PO_4, 25 mM $NaHCO_3$, and 10 mM D-glucose (pH 7.4). Small pieces of sliced tissue (~2 × 2 mm) were incubated for 45 min at 29 °C in HEPES-buffered saline (150 mM NaCl, 3 mM KCl, 2 mM $CaCl_2$, 2 mM $MgCl_2$, 10 mM HEPES, and 10 mM D-glucose (pH 7.4)) containing 19 units/ml papain. All recordings were made at room temperature (19–20 °C). Current signals from acutely isolated pyramidal cell somata recorded in whole cell voltage clamp mode were sampled at 20 kHz and filtered at 5 kHz (−3 dB) using an Axopatch 200B amplifier in conjunction with a Digidata 1322A interface and pClamp 9 software (all from Axon Instruments, Inc., Foster City, CA). Access resistance in the whole cell configuration was 10–15 megaohms before series resistance compensation (75–80%). To improve voltage control, Na^+ currents were investigated in a low Na^+ bathing solution containing 15 mM NaCl, 115 mM choline chloride, 3 mM KCl, 2 mM $MgCl_2$, 1.6 mM $CaCl_2$, 0.4 mM $CdCl_2$, 10 mM HEPES, and 10 mM D-glucose (pH 7.4). Patch pipettes were filled with 105 mM CsF, 20 mM triethanolamine chloride, 3 mM KCl, 1 mM $MgCl_2$, 8 mM HEPES, 9 mM EGTA, and 2 mM Na_2ATP (pH 7.2 adjusted with CsOH). Data are presented as means ± S.E. Data were statistically analyzed (Student's *t* test, significance set at $p < 0.05$) using Origin Pro7 software. Substances were purchased from Sigma.

Animals—A panel of 69 male mice (25 wild-type, 23 heterozygous, and 21 *bace1* knockout littermate mice, aged 3–9 months) was used to assess anxiety-related behavior in the open field test and elevated zero maze and depression-related behavior in the tail suspension test and forced swim test. Animals were individually housed and kept under a 12-h light/12-h dark cycle (lights on at 6:00 a.m.) in a temperature- and humidity-controlled room with food and water *ad libitum*. All experiments were conducted during the light phase of the light/dark cycle with 1 week between experiments.

Open Field Test—Locomotor activity was monitored using a Truscan© system (Coulbourn Instruments Inc., Allentown, PA). The animal was placed in the center of the activity field arena, which is a transparent plexiglas cage (260 (width) × 260 (depth) × 400 (height) mm) equipped with two photo beam sensor rings to register horizontal and vertical activities. Testing lasted 30 min.

Elevated Zero Maze—Elevated zero maze testing was performed as described by Crawley (30). The zero maze consists of an annular platform (diameter, 50 cm; and width, 5 cm). The animals were allowed to freely explore the maze for 5 min, and their behavior was recorded and analyzed using the Ethovision Pro video tracking system (Noldus Information Technology, Wageningen, The Netherlands).

Tail Suspension Test—Mice were suspended by their tail on a hook in a test chamber using adhesive tape. Total duration of immobility was measured over a period of 6 min using the VideoTrack system (Viewpoint, Champagne au Mont d'Or, France). Mice that curled up toward their tail or that fell off during testing were excluded from analysis.

Forced Swim Test—A mouse was placed in a cylinder (inner diameter, 10 cm) filled with water to a height of 10 cm at a temperature of 25 ± 1 °C. The mouse was exposed to swim stress for 6 min. Total duration of immobility was measured using the VideoTrack system. One animal was excluded from analysis because it had a very high fat mass and had difficulties staying afloat.

Statistical Analysis—Data were analyzed by one-way analysis of variance or by Kruskal-Wallis analysis of variance on ranks in case data were not normally distributed, followed by post hoc Tukey's test (one-way analysis of variance) or Dunn's method (Kruskal-Wallis analysis of variance on ranks) if appropriate.

RESULTS

Lethal Phenotype in bace1 Knockout Mice—Several groups have reported the generation of *bace1* knockout mice (9–11). We generated an independent line of BACE1-deficient mice (line BACE1I; supplemental "Experimental Procedures"). Briefly, a neomycin expression cassette was inserted within the first coding exon of the *bace1* gene at codon 49, resulting in the introduction of a premature in-frame translational stop codon. The absence of BACE1 protein was confirmed by Western blotting of extracts from embryonic brains using a C terminus-specific antibody against BACE1 (Fig. 1*A*). BACE1-deficient mice appeared at first glance viable and fertile. However, during expansion of the colony in two different conventional facilities in Leuven and in Kiel, we observed increased lethality among BACE1-deficient pups in the first weeks after birth. Mortality was almost exclusively restricted to the *bace1*$^{-/-}$ group (Fig. 1*B*). Of 180 *bace1* knockout pups born to *bace1* knockout parents, 34 (19%) died within the first 3–6 days of birth. Of those remaining, 44 (~24%) showed growth retardation (see, for example, Fig. 1*D*) and died by 3–4 weeks of age from a wasting syndrome. In contrast, mortality in the wild-type and heterozygous groups did not exceed 2% (Fig. 1*B*). The high neonatal death observed in *bace1*$^{-/-}$ pups was not caused by a nursing defect of BACE1-deficient mothers. In a pup exchange experiment, there was no reduction in neonatal mortality of *bace1* knockout pups born to *bace1* knockout parents when they were nursed by a wild-type mother (Fig. 1*C*). Finally, healthy *bace1* null mice were ~30% smaller by weight than control mice. This was observed in BACE1 heterozygous crosses (weight measured by 3 weeks of age, 8.3 ± 0.9 g for wild-type mice, 9.1 ± 0.4 g for *bace1*$^{+/-}$ mice, and 5.8 ± 0.4 g for *bace1*$^{-/-}$ mice) (data not shown) and further confirmed in BACE1 and BACE2 heterozygous crosses (Fig. 1*E*). The BACE1-deficient mice surviving to adulthood were fertile, and histological and anatomical examination failed to evidence any gross phenotypic abnormality (supplemental Fig. 4) (data not shown).

To exclude the possibility that mortality in our colony was due to a defect independent of BACE1 deficiency, a second BACE1-deficient line was independently generated (line BACE1II; supplemental "Experimental Procedures"). A similar mortality rate was observed with those mice (data not shown), demonstrating that mortality is directly linked to BACE1 deficiency.

BACE1 is known to cleave both PSGL-1 (P-selectin glycoprotein ligand-1) and β-galactoside α2,6-sialyltransferase I, proteins implicated in immune reactions (31–33), and therefore, we performed a series of *in vitro* and *in vivo* assays to evaluate the ability of BACE1-deficient animals to mount an efficient immune response. We first tested whether *bace1*$^{-/-}$ mice could mount an efficient immune response to vesicular stomatitis virus (VSV) infection. To this end, *bace1*$^{-/-}$ mice and heterozygous and wild-type littermates were intravenously challenged with 2 × 10^6 plaque-forming units of VSV. On day 4 after

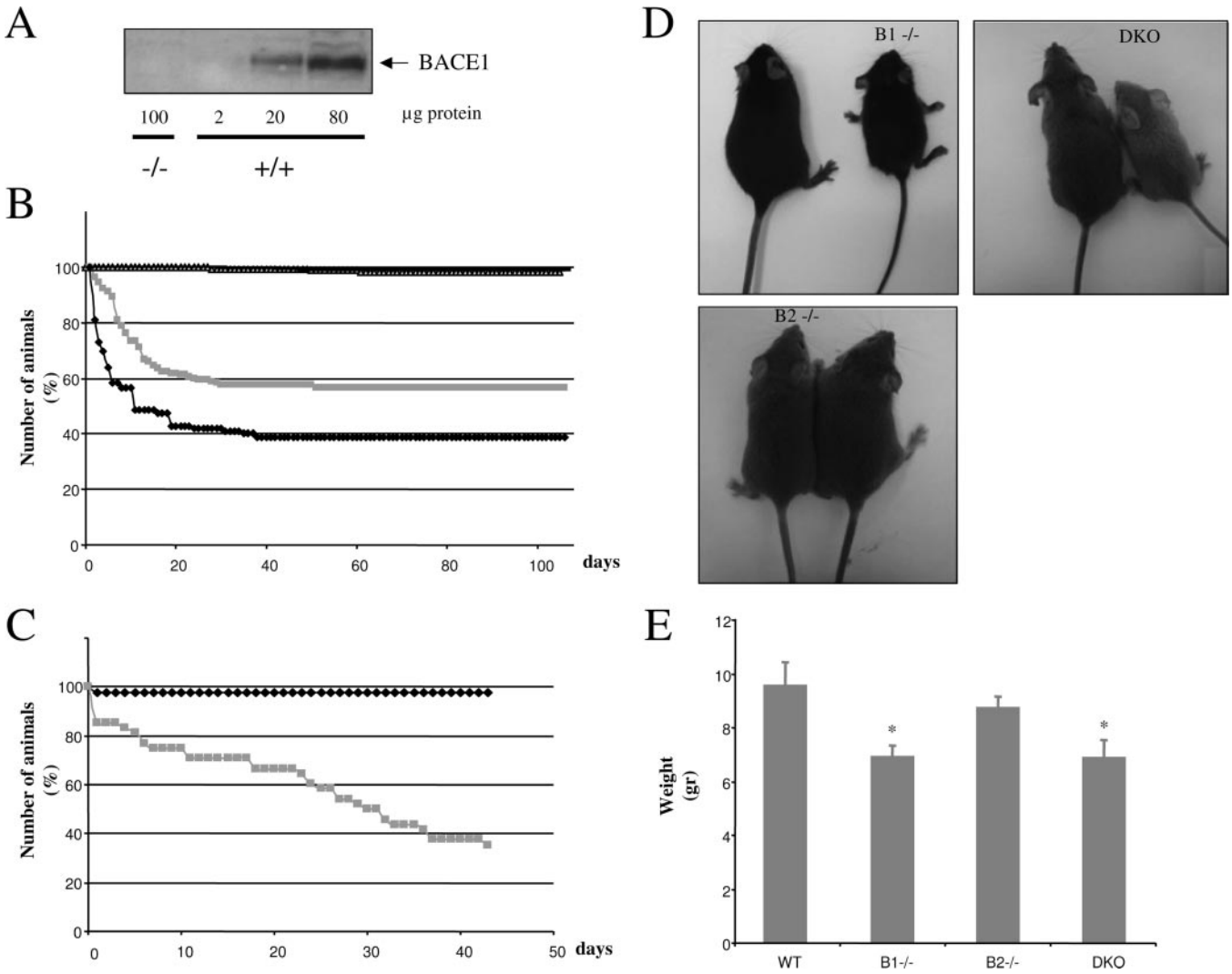

FIG. 1. **Mortality associated with BACE deficiency.** *A*: lack of BACE1 protein in brains of *bace1* knockout mice. Membrane protein extracts were prepared from day 14 embryos. Endogenous BACE1 was detected by Western blotting using the BACE1 C terminus-specific antibody B48. *B*: lethality in the *bace1* and double knockout colonies. The number of mice at birth was set as 100%. There were 180 $bace1^{-/-}$ mice (*gray squares*) derived from *bace1* knockout crosses, 122 *bace1*/*bace2* double knockout mice (*black diamonds*) derived from double knockout crosses, 232 wild-type mice (*gray triangles*), and 164 $bace1^{+/-}$ mice (*black boxes*). Mortality was almost exclusively observed in the $bace1^{-/-}$ and double knockout groups. *C*: pup exchange experiment. In this experiment, 48 *bace1* null pups born to *bace1* null parents and 42 wild-type pups born to wild-type parents were exchanged within the first day after birth. Reduction in the number of mice is expressed as a percentage of the initial number (set as 100%.). *Black diamonds*, wild-type pups nursed by *bace1* knockout mothers; *gray squares*, *bace1* null pups nursed by wild-type mothers. *D*: *upper left panel*, a 3-week-old wild-type pup (*left*) and a *bace1* knockout littermate (*right*) affected by a wasting syndrome; *upper right panel*, a $bace1^{+/+}bace2^{+/-}$ pup (*left*) and a healthy double knockout (*DKO*) littermate (*right*) by 4 weeks of age; *lower panel*, a 4-week-old *bace2* knockout pup (*left*) and a $bace1^{+/+}bace2^{+/-}$ littermate (*right*). *E*, weight (in grams) of $bace1^{+/+}bace2^{+/-}$ (wild-type (*WT*); 9.6 ± 0.9 g, $n = 16$), $bace1^{-/-}$ (6.9 ± 0.4 g, $n = 9$), $bace2^{-/-}$ (8.7 ± 0.4 g, $n = 35$), and double knockout (6.9 ± 0.7 g, $n = 11$) littermates measured by 3 weeks of age. *, $p < 0.05$ *versus* $bace1^{+/+}bace2^{+/-}$.

infection, all mice analyzed mounted similar VSV-neutralizing IgM responses that switched to the IgG isotype by day 8 and reached plateau levels at later time points (supplemental Fig. 5). Thus, adaptive immunity was functional in $bace1^{-/-}$ mice, *i.e.* VSV-neutralizing T help-independent IgM and the T help-dependent switch to the IgG subtype were normally induced. Furthermore, a similar resistance to lethal VSV infection at higher infection doses (data not shown) suggested that the overall quality and quantity of VSV-specific immunity were very similar for all genotypes. We further checked (*a*) the number and type of leukocytes that migrated into the peritoneum in a model of acute peritonitis induced by thioglycolate (34, 35), (*b*) the activation of macrophages *in vitro* as evaluated by tumor necrosis factor-α secretion upon stimulation with pathogens (*Mycobacterium avium* and *Mycobacterium tuberculosis*) or with lipopolysaccharide, and (*c*) the T-cell responses as measured by the capacity of activated T-cells isolated from spleens of preimmunized mice to destroy chromium-labeled cells from a different genetic background. All these experiments were negative (data not shown), suggesting that the overall immune defense of the *bace1* knockout animals is not dramatically compromised.

Behavioral Analysis of BACE1-deficient Mice—We tested *bace1* knockout mice (strain BACE1II) in a battery of behavioral tests (Fig. 2). In the open field test, *bace1* null mice displayed hyperactivity and enhanced locomotion compared with heterozygous and wild-type littermates, as illustrated by a significant increase in total move time ($F(2,66) = 10.743$, $p < 0.001$) (Fig. 2*A*) and total distance traveled ($H = 16.387$, $p < 0.05$) (Fig. 2*B*). The *bace1* genotype had, however, no effect on the relative time spent in the center and the relative distance traveled in the center (data not shown). This indicates that *bace1* knockout mice do not show an anxiolytic or anxiogenic phenotype, which was confirmed in the elevated zero maze test.

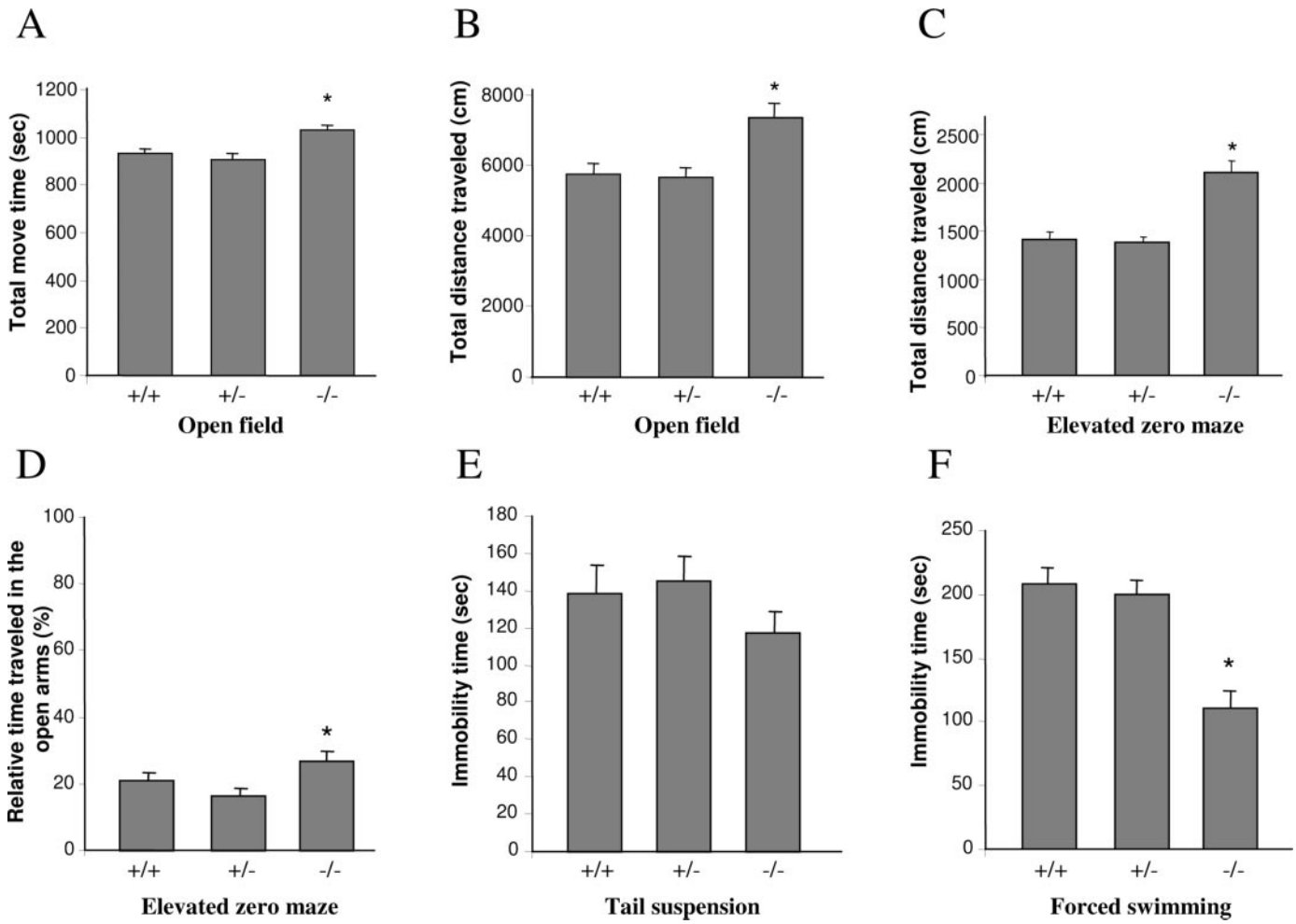

FIG. 2. **Behavioral analysis of BACE1-deficient mice.** *A* and *B*, hyperactivity and hyperlocomotion in *bace1* knockout mice in the open field test. *A*, total move time; *B*, total distance traveled. *C* and *D*, elevated zero maze test. *C*, total distance traveled; *D*, relative time spent in the open arms (time spent in the open arms/300 = duration of experiment). *E*, targeted deletion of *bace1* has no effect on depression-related behavior in the tail suspension test. *F*, *bace1* knockout mice show reduced immobility in the forced swim test. This difference probably reflects a hyperactive rather than an antidepressant phenotype. Results are presented as means ± S.E. *, $p < 0.05$ *versus* wild-type mice.

In this test, BACE1-deficient mice showed a significant increase in the total distance traveled ($F(2,65) = 21.926$, $p < 0.001$) (Fig. 2*C*), again pointing to a hyperactive phenotype. One mouse with a homozygous genotype actively jumped off the maze and was excluded from the analysis. Furthermore, there was a significant effect of genotype on the relative time spent in the open arms ($F(2,65) = 4.003$, $p = 0.023$) (Fig. 2*D*). Post hoc analysis revealed that *bace1* null mice exhibited an increase in the relative time spent in the open arms compared with heterozygous littermates ($p < 0.05$). This stresses no indication of anxiety. No influence of genotype on the relative distance traveled in the open arms could be detected (data not shown). Finally, animals were tested in the tail suspension and forced swim tests, which are both validated models for assessing depression-related behaviors. As shown in Fig. 2*E*, there was no significant effect of genotype on immobility in the tail suspension test ($F(2,59) = 1.085$, $p = 0.345$). In the forced swim test, homozygous animals showed a significant decrease in immobility time compared with heterozygous and wild-type animals ($F(2,65) = 16.625$, $p < 0.001$) (Fig. 2*F*). This difference probably reflects a hyperactive rather than an anti-depressive phenotype. Similar data were obtained in independent behavioral analyses of the BACE1I strain (data not shown).

Na^+ Currents in Cortical Neurons of bace1 Knockout Mice—BACE1 has been recently shown to cleave β_2- and β_4-subunits of voltage-gated Na^+ channels in mouse brain (36). These β-subunits are auxiliary subunits that associate with the principal pore-forming α-subunit and that regulate the function and expression of voltage-gated Na^+ channels (37). We hence wondered whether the genetic ablation of *bace1* would influence the properties of the fast Na^+ current. To address this issue, we performed whole cell recordings from pyramidal cell somata that were acutely isolated from slices of mouse neocortex. We chose this preparation because BACE1 is highly expressed in neurons of this brain region (36) and because dissociated cells offer the advantage of allowing adequate spatiotemporal voltage control of fast Na^+ currents. After pharmacological suppression of voltage-dependent Ca^{2+} and K^+ currents with Cd^{2+} and Cs^+/triethanolamine$^+$, respectively (see "Experimental Procedures"), fast Na^+ currents were gradually activated by step depolarizations to command potentials between −60 and 10 mV (Fig. 3*A*). To determine the current-voltage relationship of the Na^+ current, the peak current amplitude at each voltage step was normalized to the neuron's capacitance and plotted as a function of the command potential (Fig. 3*B*). Cortical neurons from *bace1* knockout mice had a tendency to display lower Na^+ current densities than those from wild-type mice, but this difference did not reach statistical significance. The activation curve of the Na^+ conductance (G) was constructed from the current-voltage relationship of Fig. 3*B* using the equation $G = I/(V - E_{Na})$, where I is the peak current amplitude at command potential V and E_{Na} is the

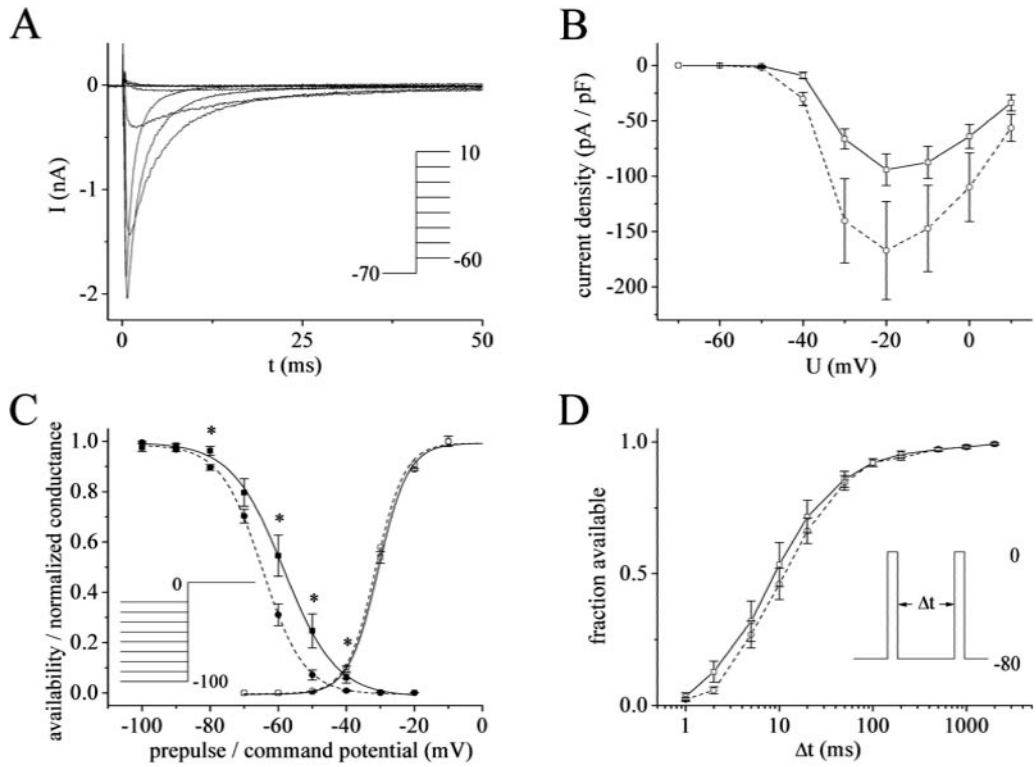

FIG. 3. **Whole cell recordings of voltage-gated Na^+ currents in acutely dissociated cortical pyramidal cells.** *A*, Na^+ current responses elicited by depolarizing voltage steps in a neuron from a *bace1* knockout mouse. The *inset* depicts the pulse protocol. *B*, normalized current-voltage curves of peak Na^+ currents in wild-type mice (*open circles*) and *bace1* knockout mice (*open squares*). *pF*, picofarads. *C*, activation (*open symbols*) and steady-state inactivation (*closed symbols*) curves of Na^+ currents in neurons from wild-type mice (*circles*) and *bace1* knockout mice (*squares*). The *inset* depicts the pulse protocol used to examine steady-state inactivation. The activation and inactivation curves were fitted by the Boltzmann equations $G/G_{max} = 1/(1 + \exp(V_h - V)/k)$ and $h_\infty = 1/(1 + \exp(V - V_h)/k)$, respectively, where V_h is the voltage of half-maximal Na^+ conductance ($G_{max}/2$) and half-maximal availability, respectively, and k is a slope factor. *, $p < 0.05$. *D*, recovery from inactivation measured using a two-pulse protocol with a variable interval (*inset*) in neurons from wild-type mice (*open circles*) and *bace1* knockout mice (*open squares*). Data points indicate the amplitude of the second Na^+ current response after normalization to the amplitude of the first response. Data in *B–D* summarize recordings from eight neurons from four wild-type mice and 10 neurons from three *bace1* knockout mice.

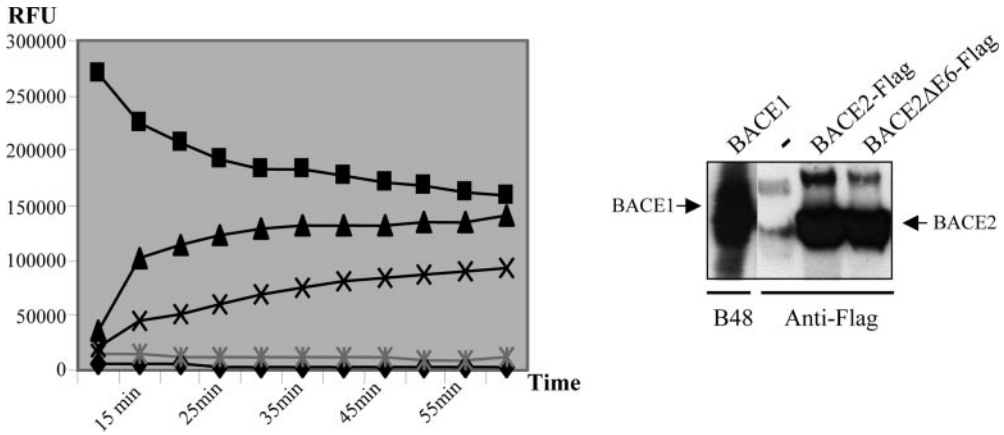

FIG. 4. **BACE2ΔE6 protein is inactive in a β-secretase *in vitro* assay.** Shown are the results from fluorescence resonance energy transfer analysis of immunopurified BACE1, BACE2-FLAG, and BACE2Δ6-FLAG using a peptide based on the Swedish APP mutation. The peptide carries a fluorescence donor at one end and a quencher acceptor at the other. The intact substrate is therefore weakly fluorescent, but becomes highly fluorescent upon enzymatic cleavage. Although both BACE1 and BACE2 efficiently cleaved the substrate, there was no activity associated with the BACE2ΔE6 protein (*left panel*). Western blot analysis of immunoprecipitated proteins demonstrated that similar amounts of input material were tested (*right panel*). *Black diamond*, substrate alone; *black square*, 100% product; *black triangle*, BACE1; *black* ×, BACE2-FLAG; *gray* ×, BACE2Δ6-FLAG. *RFU*, relative fluorescence units.

equilibrium potential for Na^+ under our experimental conditions. As shown in Fig. 3*C* (*open symbols*), the activation curve of the Na^+ conductance did not differ between neurons from wild-type and *bace1*$^{-/-}$ mice. Steady-state inactivation of Na^+ currents was determined by holding the neuron for 1 s at prepulse potentials between −100 and −20 mV before evoking a Na^+ current response with a voltage step to 0 mV. Current amplitudes were expressed as a fraction of the maximal current amplitude and plotted as a function of the prepulse potential. In contrast to activation, steady-state inactivation did vary significantly between neurons from wild-type and BACE1-deficient mice (Fig. 3*C*, *closed symbols*). The rightward shift of the steady-state inactivation curve in neurons from BACE1-deficient mice (wild-type mice, $V_h = -65$ mV (*dashed curve*); and

bace1 knockout mice, $V_h = -58$ mV (*solid curve*)) indicates that a larger fraction of Na^+ channels is available at a given potential compared with neurons from wild-type mice. Recovery from inactivation was studied by gradually increasing the interval (1 ms to 2 s) between two 15-ms test pulses to 0 mV. The peak amplitude of the second Na^+ current response divided by the response at the maximal interval was then plotted as a function of the interpulse interval. As shown in Fig. 3*D*, recovery from inactivation was not significantly different between the two groups.

Generation and Characterization of bace2 Knockout Mice—To understand the *in vivo* function of the β-secretase homolog BACE2, a *bace2* knockout mouse line was generated. Two *loxP* sites were first introduced in the introns flanking exon 6, which contains one of the two active sites of the enzyme. Mice heterozygous for the *bace2* conditional targeted allele were subsequently crossed with mice expressing Cre recombinase from the ubiquitous phosphoglycerate kinase promoter, resulting in the deletion of *bace2* exon 6 (BACE2ΔE6) (supplemental "Experimental Procedures"). To demonstrate that the BACE2ΔE6 protein does not have β-secretase activity, BACE1, BACE2, and BACE2ΔE6 expressed in COS cells were immunoprecipitated from cell extracts, and protease activity was measured in an *in vitro* assay using a synthetic peptide representing the BACE1 cleavage site of APPsw. Only BACE1 and BACE2 (but not BACE2ΔE6) were capable of cleaving the peptide (Fig. 4). Western blotting confirmed that similar levels of BACE2 and BACE2ΔE6 were tested in the assay (Fig. 4). Thus, the BACE2ΔE6 protein encoded in *bace2* knockout mice lacks protease activity.

Mice homozygous for the deficient *bace2* allele were born at normal frequency and were fertile and healthy overall. No difference in size could be identified when compared with littermate controls (Fig. 1, *D* and *E*). In a standard battery of blood and clinical chemistry parameters, no abnormality associated with the genotype was detected (data not shown). Extensive pathological analysis of four $bace2^{+/+}$ and four $bace2^{-/-}$ mice with hematoxylin and eosin staining failed to show any abnormality related to genotype (supplemental "Experimental Procedures").

Generation and Characterization of $bace1^{-/-}bace2^{-/-}$ *Knockout Mice*—To identify putative major BACE functions that could be compensated for in the single monogenic *bace* knockout lines, we generated mice deficient in both BACE1 and BACE2 proteases. Interestingly, double knockout mice had a neonatal mortality of ~60%, which was higher than that observed in the single BACE1-deficient line (Fig. 1*B*). Of 122 double knockout mice born to double knockout parents, 51 (~42%) died within the first 3–5 post-natal days. An additional 24 pups (~20%) died within the first 3–4 weeks from a wasting syndrome. The surviving animals were fertile, and a detailed pathological examination failed to reveal any abnormality (supplemental "Experimental Procedures") (data not shown). Like *bace1* knockout mice, healthy double knockout animals remained smaller than their control littermates (Fig. 1, *D* and *E*).

Processing of APP in BACE-deficient Cells—We next analyzed the processing of APP in cells derived from knockout animals. We started with primary neurons because, although BACE1 is expressed at relatively high levels in neurons, BACE2 expression in these cells is still a matter of debate (2, 13, 19). We analyzed in parallel APPwt, APPsw, and APPfl. APPsw and APPfl were chosen because both mutations are known to affect β-secretase cleavage (8).

We confirmed that BACE1-deficient neurons do not process APP at the known β-secretase sites (Asp^1 and Glu^{11}) as shown by the absence of β1 and β11 C-terminal fragments (Fig. 5*A*).

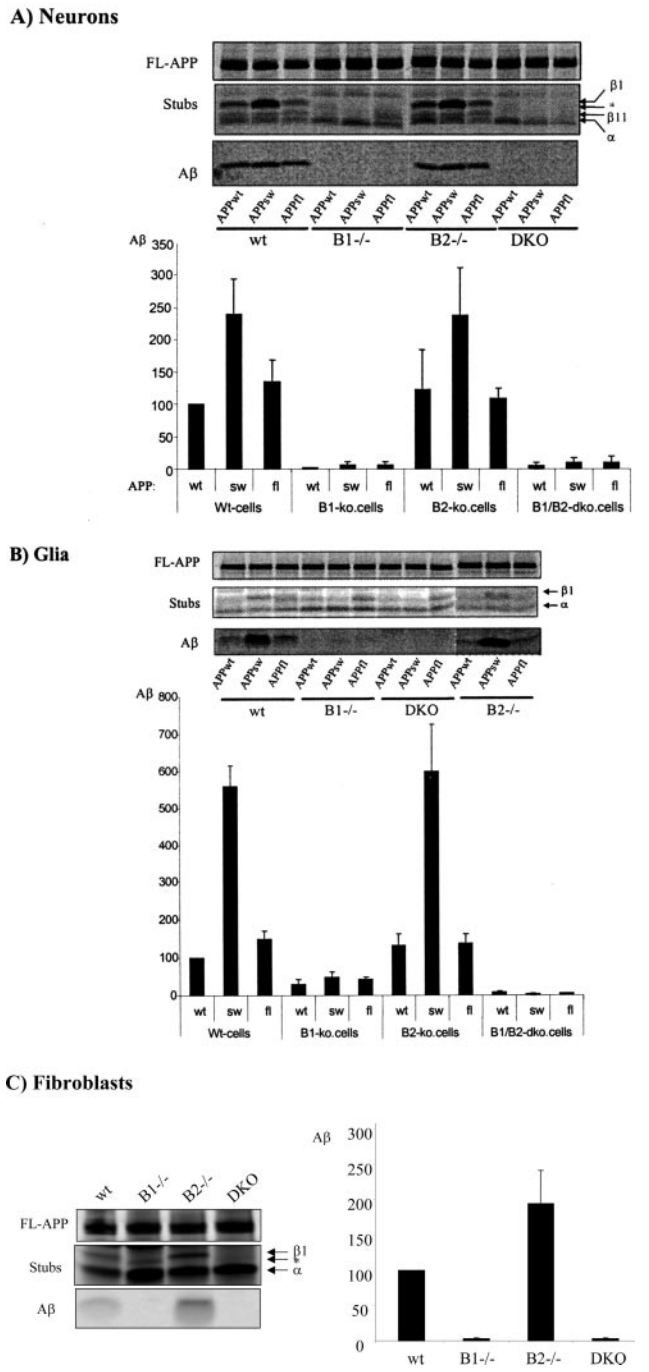

FIG. 5. **Analysis of APP processing in cells derived from BACE-deficient mice.** Primary cortical neurons (*A*) and glial cells (*B*) were prepared from day 14 embryos and infected with recombinant SFV encoding APPwt, APPsw, or APPfl. Cells were metabolically labeled with [^{35}S]methionine for 4 h, and full-length APP (*FL-APP*) and C-terminal fragments (*Stubs*) were immunoprecipitated from a cell extract using antibody B63. Aβ was immunoprecipitated from the conditioned medium with antibody B7/8. The levels of secreted Aβ were quantified by PhosphorImager analysis and are expressed relative to the levels of full-length APP. The level of Aβ secreted by wild-type (*wt*) cells upon expression of APPwt was fixed as 100%. Results are presented as means ± S.E. *DKO*, double knockout; *ko*, knockout. Mouse fibroblasts were derived from the peritonea and diaphragms of adult mice and immortalized by stable expression of the SV40 large T antigen (*C*). Fibroblasts were transduced with recombinant adenovirus expressing APPsw. Processing of APP was analyzed as described under "Experimental Procedures." All experiments were performed at least three times.

However, we observed a novel APP C-terminal fragment that migrated slightly faster than the β1 C-terminal fragment (Fig. 5*A*, *asterisk*). BACE2 is not responsible for this cleavage be-

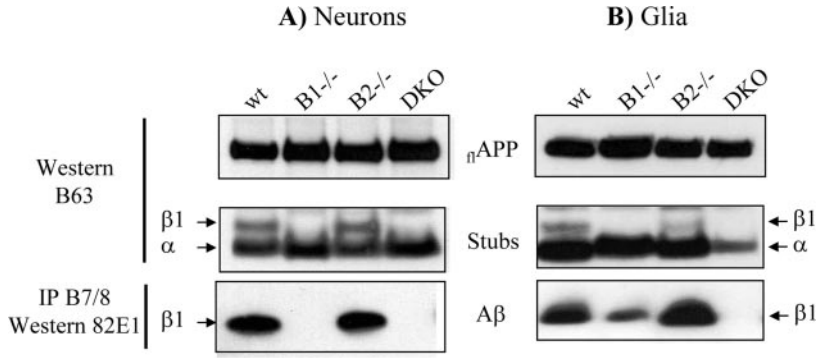

FIG. 6. **Analysis of APP processing using the Aβ N terminus-specific antibody 82E1.** Primary cortical neurons (*A*) and glial cells (*B*) were infected with recombinant SFV encoding APPwt and APPsw, respectively. Samples of cell extract were probed with the APP C terminus-specific antibody B63 to detect full-length APP (*flAPP*; *upper panels*) and APP C-terminal fragments (*stubs*; *middle panels*). Aβ was immunoprecipitated (*IP*) from the conditioned medium with antibody B7/8 and detected with antibody 82E1 (*lower panels*). *wt*, wild-type; *DKO*, double knockout.

cause the same fragment was still produced in double BACE1/BACE2-deficient neurons. The facts that *bace1* knockout neurons did not produce any measurable Aβ and that there was no measurable effect on APP processing in primary neurons deficient in BACE2 confirm that BACE1 is the only β-secretase in these cells. Glial cells are the most abundant cells in brain, and we next investigated how APP processing is affected by the absence of BACE proteases. Interestingly, BACE1-deficient glial cells secreted measurable levels of Aβ, which were more prominent in APPsw- and APPfl-transduced cells (Fig. 5*B*). Moreover, although wild-type cells overexpressing APPsw produced about four times higher levels of Aβ compared with APPfl-overexpressing cells, the situation changed in BACE1-deficient cells. In this case, similar amounts of Aβ were generated by the APPsw and APPfl mutants, and the amounts generated by these mutants were slightly higher than those produced by APPwt-expressing glial cells. This is consistent with BACE2 being the responsible protease because it has been shown that the Flemish mutation in APP markedly increases Aβ production by BACE2 (8). That BACE2 contributes to Aβ generation in cultured glial cells is also demonstrated by the fact that, in BACE1-deficient glial cells, we observed significant Aβ generation, which was reduced to undetectable levels only in the combined BACE1/BACE2 deficiency. These data suggest that BACE2 is expressed in glial cells and might contribute to Aβ production *in vivo* in these cells.

To demonstrate that the Aβ measured in these experiments was generated by cleavage at the authentic β-secretase site, we made use of antibody 82E1, which specifically recognizes the neoepitope produced upon BACE cleavage of APP at Asp^1 (38). Similar to the results described above, BACE1-deficient glial cells (but not neurons) continued to generate Aβ detected by antibody 82E1 (Fig. 6), demonstrating that the observed cleavage was carried out by a β-secretase.

Finally, we analyzed processing of APPsw in fibroblasts derived from BACE-deficient mice (Fig. 5*C*). Analogous to neuronal cells, there was a compensatory cleavage of APP in *bace1* knockout fibroblasts that resulted in the generation of a C-terminal fragment similar to that observed in neurons. Double knockout cells still produced this fragment, demonstrating that, as in neurons, BACE2 is not responsible for this compensatory cleavage. Interestingly, fibroblasts deficient in the BACE2 enzyme secreted higher levels of Aβ compared with wild-type cells. These results indicate that fibroblast endogenous BACE2 has an anti-amyloidogenic function *in vivo*.

DISCUSSION

We generated mouse lines that are deficient in BACE1, BACE2, or both. Previous reports claimed that genetic ablation of *bace1* does not result in overt phenotypic alterations (9–11, 39). One group reported a more timid, more anxious, and less exploratory behavior in these mice (40). In contrast, we found a complex but significant phenotype in our two independently generated *bace1* knockout strains, which are characterized by increased neonatal mortality affecting up to ~40% of newborn animals. The surviving mice were healthy and fertile, but displayed a lower weight. They showed also hyperactivity and enhanced locomotion in a battery of behavioral tests. The phenotype of BACE2-deficient mice has not been reported previously. We found thus far no indications of any physiological or anatomical abnormalities when the animals were kept under similar breeding conditions as our BACE1 strains. This is somewhat surprising because BACE2 is ubiquitously expressed in fetal and adult tissues (12), and further work is needed to determine more precisely the physiological role of BACE2. The increased neonatal mortality observed in *bace1*/*bace2* double knockout mice compared with single BACE1 deficiency indicates, however, that at least some overlap exists between BACE1 and BACE2 functions. It is unclear at the moment why one group of *bace1* and double knockout mice died within the first weeks after birth, whereas others survived into adulthood. Possible explanations for this diversity include effects of modifier genes and varying levels of compensatory contributions from other (related) genes. Mortality seems to be associated with an environmentally born factor that triggers death only in combination with BACE1 deficiency. This probably explains why other groups did not observe mortality in their $bace1^{-/-}$ strains and is supported by the fact that the BACE1II line presented neonatal mortality only when the animals were housed in the same facility as the BACE1I line, but not in the specific pathogen-free facility where they originally came from (data not shown). Because BACE1 is known to cleave both PSGL-1 and β-galactoside α2,6-sialyltransferase I, proteins implicated in immune reactions (31–33), we speculated that the higher mortality rate observed in *bace1* knockout mice might reflect a deficient immune response in a non-pathogen-free environment. The analyses we performed thus far (see "Results") failed, however, to reveal any defect of *bace1* knockout mice in their capacity to mount an efficient immune response. We excluded also the possibility that *bace1* knockout mothers are deficient in milk production or do not care for their pups by performing pup exchange experiments (Fig. 1*C*). Because the lethality rate did not decrease when the knockout pups were nursed by wild-type mothers and because no lethality was observed when BACE1-deficient mothers nursed wild-type pups, we conclude that the lethality problem is linked with BACE1 deficiency in the pups. Because the adult mice displayed an abnormal hyperactive behavior (Fig. 2), it remains an interesting speculation that behavioral alterations in the pups could contribute to lethality. There are, however, no behavioral tests available for newborn mice to evaluate this possibility in further detail.

It was recently shown that BACE1 cleaves the β-subunits of voltage-gated sodium channels (36). The β-subunits belong to the immunoglobulin superfamily of cell adhesion molecules,

and besides their cell adhesion function, they play a role in channel gating and cell-surface expression of the pore-forming α-subunits (41). Given the prominent expression of BACE1 in the striatum (36), it is tempting to speculate that changes in Na^+ channel function might contribute to the hyperactive phenotype of *bace1* null mice reported in this study. We checked this by performing whole cell recordings from cortical neurons. We found that the lack of BACE1 was associated with a significant shift in steady-state inactivation of the Na^+ current toward more depolarized potentials. In contrast, the voltage dependence of activation was not altered. The shift in steady-state inactivation might be functionally important because it increases the availability of Na^+ channels in the critical voltage range around the firing threshold. In addition to modulating Na^+ currents, BACE might also regulate synaptic function. Kamenetz *et al.* (42) recently proposed a feedback loop in which Aβ plays a prominent role. According to their model, an increase in neuronal activity induces BACE1, leading to enhanced production of Aβ, which in turn depresses excitatory synaptic transmission. Thus, blockade of BACE1 might be expected to influence neuronal excitability at both the cellular and neuronal network levels, and such alterations might manifest as the subtle behavioral deficits observed in BACE1-deficient mice. Again, further work is needed to firmly establish cause-consequence relationships in this regard.

We finally analyzed in detail the role of BACE1 and BACE2 in APP processing. We have confirmed that BACE1 is the major β-secretase *in vivo* and is basically the only β-secretase that is active in neurons. Interestingly, cultured glial cells derived from *bace1* knockout mice still secreted in the conditioned medium measurable amounts of an Aβ-like peptide. This peptide was no longer detected in double BACE1/BACE2-deficient glial cells, demonstrating that BACE2 is expressed in these cells and raising the intriguing possibility that glia-expressed BACE2 contributes to the total brain Aβ pool. This could be particularly relevant in Down syndrome because the *bace2* gene (like the APP gene) is located on chromosome 21 (21). Also, some mutations in APP (like the Flemish APP familial Alzheimer disease mutation) increase BACE2-dependent Aβ production (Fig. 5*B*) (8). That the observed protein band was authentic Aβ was confirmed using the highly specific monoclonal antibody 82E1 (38), which reacts with the neoepitope generated by BACE1 cleavage at position 1 of Aβ (Fig. 6). Interestingly, the effects of BACE2 on APP processing appear to be cell type-specific. For instance, in fibroblast cells, BACE2 appears to prevent Aβ generation because BACE2-deficient fibroblasts generated higher levels of Aβ compared with their wild-type littermates (Fig. 5).

In conclusion, this work has addressed the important question of the physiological role of BACE1 and BACE2. It is obvious that the functions of these two proteases are quite subtle and that the molecular link between the observed phenotype and BACE1 deficiency remains to be firmly established. We will now use these mice for further detailed molecular analysis, hoping that identifying additional substrates of BACE1 and BACE2 will help to elucidate the full functional importance of these proteases and provide further insight into the phenotype of the mice. Although our data do not necessarily contradict the current assumption that BACE1 is a valid drug target to treat AD, they bring up a cautionary note to the prevailing optimism based on previous studies that stressed the normal phenotype of *bace1* null mice. Obviously, in the absence of a complete understanding of the functions of BACE, it remains a problem to make predictions with regard to the outcome of BACE inhibition in humans. We conclude already, however, that a detailed observation of the impact of BACE inhibitors on behavior is indicated. It remains nevertheless surprising that ~40% of mice with a combined absence of BACE1 and BACE2 can indeed survive for >1.5 years under what seems to be quite healthy and fertile conditions.

Acknowledgments—We thank Dr. Noriaki Kinoshita (IBL Co., Ltd.) for kindly providing antibody 82E1, Dr. Wim Annaert (Katholieke Universiteit Leuven) and Dr. Collin Dingwall (GlaxoSmithKline) for contributing anti-BACE antibodies, Dr. Norbert Reiling for helping analyze macrophage function, and Marlies Rusch for technical assistance.

REFERENCES

1. Hussain, I., Powell, D., Howlett, D. R., Tew, D. G., Meek, T. D., Chapman, C., Gloger, I. S., Murphy, K. E., Southan, C. D., Ryan, D. M., Smith, T. S., Simmons, D. L., Walsh, F. S., Dingwall, C., and Christie, G. (1999) *Mol. Cell. Neurosci.* **14,** 419–427
2. Hussain, I., Powell, D. J., Howlett, D. R., Chapman, G. A., Gilmour, L., Murdock, P. R., Tew, D. G., Meek, T. D., Chapman, C., Schneider, K., Ratcliffe, S. J., Tattersall, D., Testa, T. T., Southan, C., Ryan, D. M., Simmons, D. L., Walsh, F. S., Dingwall, C., and Christie, G. (2000) *Mol. Cell. Neurosci.* **16,** 609–619
3. Sinha, S., Anderson, J. P., Barbour, R., Basi, G. S., Caccavello, R., Davis, D., Doan, M., Dovey, H. F., Frigon, N., Hong, J., Jacobson-Croak, K., Jewett, N., Keim, P., Knops, J., Lieberburg, I., Power, M., Tan, H., Tatsuno, G., Tung, J., Schenk, D., Seubert, P., Suomensaari, S. M., Wang, S., Walker, D., and John, V. (1999) *Nature* **402,** 537–540
4. Vassar, R., Bennett, B. D., Babu-Khan, S., Kahn, S., Mendiaz, E. A., Denis, P., Teplow, D. B., Ross, S., Amarante, P., Loeloff, R., Luo, Y., Fisher, S., Fuller, J., Edenson, S., Lile, J., Jarosinski, M. A., Biere, A. L., Curran, E., Burgess, T., Louis, J. C., Collins, F., Treanor, J., Rogers, G., and Citron, M. (1999) *Science* **286,** 735–741
5. Yan, R., Bienkowski, M. J., Shuck, M. E., Miao, H., Tory, M. C., Pauley, A. M., Brashier, J. R., Stratman, N. C., Mathews, W. R., Buhl, A. E., Carter, D. B., Tomasselli, A. G., Parodi, L. A., Heinrikson, R. L., and Gurney, M. E. (1999) *Nature* **402,** 533–537
6. Lin, X., Koelsch, G., Wu, S., Downs, D., Dashti, A., and Tang, J. (2000) *Proc. Natl. Acad. Sci. U. S. A.* **97,** 1456–1460
7. Acquati, F., Accarino, M., Nucci, C., Fumagalli, P., Jovine, L., Ottolenghi, S., and Taramelli, R. (2000) *FEBS Lett.* **468,** 59–64
8. Farzan, M., Schnitzler, C. E., Vasilieva, N., Leung, D., and Choe, H. (2000) *Proc. Natl. Acad. Sci. U. S. A.* **97,** 9712–9717
9. Cai, H., Wang, Y., McCarthy, D., Wen, H., Borchelt, D. R., Price, D. L., and Wong, P. C. (2001) *Nat. Neurosci.* **4,** 233–234
10. Roberds, S. L., Anderson, J., Basi, G., Bienkowski, M. J., Branstetter, D. G., Chen, K. S., Freedman, S. B., Frigon, N. L., Games, D., Hu, K., Johnson-Wood, K., Kappenman, K. E., Kawabe, T. T., Kola, I., Kuehn, R., Lee, M., Liu, W., Motter, R., Nichols, N. F., Power, M., Robertson, D. W., Schenk, D., Schoor, M., Shopp, G. M., Shuck, M. E., Sinha, S., Svensson, K. A., Tatsuno, G., Tintrup, H., Wijsman, J., Wright, S., and McConlogue, L. (2001) *Hum. Mol. Genet.* **10,** 1317–1324
11. Luo, Y., Bolon, B., Kahn, S., Bennett, B. D., Babu-Khan, S., Denis, P., Fan, W., Kha, H., Zhang, J., Gong, Y., Martin, L., Louis, J. C., Yan, Q., Richards, W. G., Citron, M., and Vassar, R. (2001) *Nat. Neurosci.* **4,** 231–232
12. Solans, A., Estivill, X., and de La Luna, S. (2000) *Cytogenet. Cell Genet.* **89,** 177–184
13. Bennett, B. D., Babu-Khan, S., Loeloff, R., Louis, J. C., Curran, E., Citron, M., and Vassar, R. (2000) *J. Biol. Chem.* **275,** 20647–20651
14. Pike, C. J., Overman, M. J., and Cotman, C. W. (1995) *J. Biol. Chem.* **270,** 23895–23898
15. Masters, C. L., Simms, G., Weinman, N. A., Multhaup, G., McDonald, B. L., and Beyreuther, K. (1985) *Proc. Natl. Acad. Sci. U. S. A.* **82,** 4245–4249
16. Naslund, J., Schierhorn, A., Hellman, U., Lannfelt, L., Roses, A. D., Tjernberg, L. O., Silberring, J., Gandy, S. E., Winblad, B., and Greengard, P., Nordstedt, C., and Terenius, L. (1994) *Proc. Natl. Acad. Sci. U. S. A.* **91,** 8378–8382
17. Fluhrer, R., Capell, A., Westmeyer, G., Willem, M., Hartung, B., Condron, M. M., Teplow, D. B., Haass, C., and Walter, J. (2002) *J. Neurochem.* **81,** 1011–1020
18. Yan, R., Munzner, J. B., Shuck, M. E., and Bienkowski, M. J. (2001) *J. Biol. Chem.* **276,** 34019–34027
19. Basi, G., Frigon, N., Barbour, R., Doan, T., Gordon, G., McConlogue, L., Sinha, S., and Zeller, M. (2003) *J. Biol. Chem.* **278,** 31512–31520
20. Wong, P. C., Price, D. L., and Cai, H. (2001) *Science* **293,** 1434
21. Motonaga, K., Itoh, M., Becker, L. E., Goto, Y., and Takashima, S. (2002) *Neurosci. Lett.* **326,** 64–66
22. Wong, G. T., Manfra, D., Poulet, F. M., Zhang, Q., Josien, H., Bara, T., Engstrom, L., Pinzon-Ortiz, M. C., Fine, J. S., Lee, H. J., Zhang, L., Higgins, G. A., and Parker, E. M. (2004) *J. Biol. Chem.* **279,** 12876–12882
23. Tournoy, J., Bossuyt, X., Snellinx, A., Regent, M., Garmyn, M., Serneels, L., Saftig, P., Craessaerts, K., De Strooper, B., and Hartmann, D. (2004) *Hum. Mol. Genet.* **13,** 1321–1331
24. Ohno, M., Sametsky, E. A., Younkin, L. H., Oakley, H., Younkin, S. G., Citron, M., Vassar, R., and Disterhoft, J. F. (2004) *Neuron* **41,** 27–33
25. De Strooper, B., Simons, M., Multhaup, G., Van Leuven, F., Beyreuther, K., and Dotti, C. G. (1995) *EMBO J.* **14,** 4932–4938
26. Esselens, C., Oorschot, V., Baert, V., Raemaekers, T., Spittaels, K., Serneels, L., Zheng, H., Saftig, P., De Strooper, B., Klumperman, J., and Annaert, W. (2004) *J. Cell Biol.* **166,** 1041–1054
27. Simons, M., De Strooper, B., Multhaup, G., Tienari, P. J., Dotti, C. G., and Beyreuther, K. (1996) *J. Neurosci.* **16,** 899–908
28. Tienari, P. J., De Strooper, B., Ikonen, E., Ida, N., Simons, M., Masters, C. L.,

Dotti, C. G., and Beyreuther, K. (1996) *Cold Spring Harbor Symp. Quant. Biol.* **61,** 575–585
29. Alzheimer, C. (1994) *J. Physiol.* (*Lond.*) **479,** 199–205
30. Crawley, J. N. (2000) *What's Wrong with My Mouse? Behavioral Phenotyping of Transgenic and Knockout Mice*, John Wiley & Sons, Inc., New York
31. Yang, J., Hirata, T., Croce, K., Merrill-Skoloff, G., Tchernychev, B., Williams, E., Flaumenhaft, R., Furie, B. C., and Furie, B. (1999) *J. Exp. Med.* **190,** 1769–1782
32. Xia, L., Sperandio, M., Yago, T., McDaniel, J. M., Cummings, R. D., Pearson-White, S., Ley, K., and McEver, R. P. (2002) *J. Clin. Investig.* **109,** 939–950
33. Hennet, T., Chui, D., Paulson, J. C., and Marth, J. D. (1998) *Proc. Natl. Acad. Sci. U. S. A.* **95,** 4504–4509
34. Tedder, T. F., Steeber, D. A., and Pizcueta, P. (1995) *J. Exp. Med.* **181,** 2259–2264
35. Watson, S. R., Fennie, C., and Lasky, L. A. (1991) *Nature* **349,** 164–167
36. Wong, H. K., Sakurai, T., Oyama, F., Kaneko, K., Wada, K., Miyazaki, H., Kurosawa, M., De Strooper, B., Saftig, P., and Nukina, N. (2005) *J. Biol. Chem.* **280,** 23009–23017
37. Isom, L. L. (2002) *Front. Biosci.* **7,** 12–23
38. Qi-Takahara, Y., Morishima-Kawashima, M., Tanimura, Y., Dolios, G., Hirotani, N., Horikoshi, Y., Kametani, F., Maeda, M., Saido, T. C., Wang, R., and Ihara, Y. (2005) *J. Neurosci.* **25,** 436–445
39. Luo, Y., Bolon, B., Damore, M. A., Fitzpatrick, D., Liu, H., Zhang, J., Yan, Q., Vassar, R., and Citron, M. (2003) *Neurobiol. Dis.* **14,** 81–88
40. Harrison, S. M., Harper, A. J., Hawkins, J., Duddy, G., Grau, E., Pugh, P. L., Winter, P. H., Shilliam, C. S., Hughes, Z. A., Dawson, L. A., Gonzalez, M. I., Upton, N., Pangalos, M. N., and Dingwall, C. (2003) *Mol. Cell. Neurosci.* **24,** 646–655
41. Isom, L. L. (2002) *Novartis Found. Symp.* **241,** 124–138; discussion 138–143, 226–132
42. Kamenetz, F., Tomita, T., Hsieh, H., Seabrook, G., Borchelt, D., Iwatsubo, T., Sisodia, S., and Malinow, R. (2003) *Neuron* **37,** 925–937

Phenotypic and Biochemical Analyses of BACE1- and BACE2-deficient Mice

Diana Dominguez, Jos Tournoy, Dieter Hartmann, Tobias Huth, Kim Cryns, Siska Deforce, Lutgarde Serneels, Ira Espuny Camacho, Els Marjaux, Katleen Craessaerts, Anton J. M. Roebroek, Michael Schwake, Rudi D'Hooge, Patricia Bach, Ulrich Kalinke, Dieder Moechars, Christian Alzheimer, Karina Reiss, Paul Saftig and Bart De Strooper

J. Biol. Chem. 2005, 280:30797-30806.
doi: 10.1074/jbc.M505249200 originally published online June 29, 2005
